JOURNAL OF MATERIALS SCIENCE 19 (1984) 1876–1884

X-ray structural analysis of activated silica

Z. BOCHYŃSKI, M. STACHOWIAK
Electron and X-Ray Diffraction Group, Institute of Physics, Adam Mickiewicz University, 60-780 Poznań 2, Grunwaldzka 6, Poland

S. MOCYDLARZ
Institute of Chemical Technology, Poznań Technical University, 60-965 Poznań 1, Mary Skłodowska-Curie Square 1, Poland

The structure of silica activated by different substituents/activators, R_n (Table I) was analysed by the method of radial distribution functions. The structural parameters of the space configuration of silica were determined beforehand. Fourier analysis of the angular distribution of X-ray radiation supports the existence of a tetrahedral configuration of silicon with respect to oxygen in a silica of the $SiO_2 + R_n$ type. The preliminary analysis makes grounds for further quantitative analysis, which permits the construction of a structural model of pure and activated silica with the activators built in it, and quantitative analysis of the local ordering degree in larger areas. Further specification of the structural parameters obtained by radial distribution functions [1], and of the parameters of long-range ordering obtained in the method of small-angle diffusion by Guinier analysis, are the next stage of the studies of approximation of the real structure of the analysed noncrystalline system, and are discussed in subsequent papers [1].

1. Introduction

This paper should be treated as an introduction in the attempts to apply radial distribution functions in the analysis of structure of a noncrystalline system which, for example, is silica activated with various activators.

Radial distribution function methods are applied. The radial distributions are obtained by numerical analysis, applying digital computer methods to experimental angular functions of intensity distribution, $\bar{I}(\theta)$ (with all corrections included, and afterwards normalization of the curves [2–4]) with the help of the Fourier transform of the function, $\bar{I}(\theta)$ [4, 5].

In the studies silica of one kind was used, obtained chemically and activated in such a way that its chemical composition did not change in 97 to 98% mass fraction. Only vestigial amounts of silica, 2 to 3 mass fraction (percentage by weight), formed a stable system with an activator, R_n, which corresponded approximately to the chemical structure of the compound presented in Table I. Thus, we attempted to determine the differences in structure of individual kinds of activated silica and the differences between the activated and nonactivated pure silica.

In the production of loaded pure gum compounds the fillers used are reinforcing carbon black and silica.

The amount of filler used in pure gum compounds is about 40% mass fraction and hence the increase in its price significantly influences the final price of the product. In the face of this situation we have started to look for new fillers which have a stable price and low production costs.

The systematic studies performed revealed that the filler which meets these requirements is the waste silica from the production of aluminium fluoride and hydrofluoric acid, after proper activation. Our studies were performed on the waste silica formed in the process of production of aluminium fluoride. This silica has the structure appropriate to perform the activation process in result of which a layer of an activator is formed on the surface. This layer is an intermediate substance connecting the filler with the polymer.

0022–2461/84 $03.00 + .12 © 1984 Chapman and Hall Ltd.

TABLE I Structural formulae and concentration of activators in the silica series studied

Preparation number, *n*	Preparation symbol	Structure of molecule with activation group, R_n	Activation group, R_n	Concentration of molecules with activation groups in silica	Elongation (%)	Mechanical resistance (kg cm^{-2})	Remarks
1	A-001	$SiO_2 + R_1$	$R_1 = CH_3(CH_2)_5 \cdot SH$	2–3%	435	176	chemically activated silica silica of stable with a filler
2	A-002	$SiO_2 + R_2$	$R_2 = (CH_3)_4 \cdot Si$	2–3%	512	139	
3	A-003	$SiO_2 + R_3$	$R_3 = NH_2 \cdot CH_2 \cdot CH_2 \cdot NHCH_2 \cdot CH_2 \cdot CH_2 \cdot Si(OCH_3)_3$	2–3%	490	145	
4	A-004	$SiO_2 + R_4$	$R_4 = NH_2 \cdot CH_2 \cdot CH_2 \cdot CH_2 \cdot Si(OC_2H_5)_3$	2–3%	420	155	
5	A-005	$SiO_2 + R_5$	$R_5 = HSCH_2 \cdot CH_2 \cdot CH_2 \cdot Si(OCH_3)_3$	2–3%	380	175	
6	A-006	$SiO_2 + R_6$	$R_6 = NH_2 \cdot CH_2 \cdot CH_2 \cdot NHCH_2 \cdot CH_2 \cdot CH_2 \cdot Si(OCH_3)_3$	2–3%	490	145	
7	A-007	$SiO_2 + R_7$	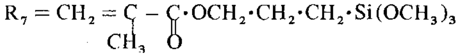 $R_7 = CH_2 = \underset{CH_3}{C} - \underset{\parallel \atop O}{C} \cdot OCH_2 \cdot CH_2 \cdot CH_2 \cdot Si(OCH_3)_3$	2–3%	575	121	
8	A-008	SiO_2 non-activated	$R_8 = 0$	0	538	65	non-activated silica

The purpose of our work is to perform direct analysis of the internal structure of pure and activated silica obtained on a semitechnical scale. This analysis is performed by wide and, in part, small-angle X-ray diffraction [6, 7]. The purpose of the studies was to find characteristic parameters of internal structure and their space distributions (i.e. the mean interatomic and intermolecular distances, number of atoms in coordination sphere, kind of packing and steric constraints in local groups of higher symmetry).

In the aperiodic nodal lattice [6–8] which can be ascribed to inorganic oxide glass, to silica studies and even to molecular liquids [8], local regions of mutually ordered configuration of atoms occur [9, 10]. These regions of mutually ordered configuration of atoms occur [9, 10]. These regions formed of the atoms arranged in groups or complexes are characterized by ordering degree and local symmetry higher than that of the surroundings. Mean dimensions of the analysed groups occurring in the structure of silica can be determined from the function of broad and especially small-angle X-ray diffusion by Fourier analysis.

Structural analysis was performed for the series of chemically activated silica and for pure silica which was the reference compound. Its molecule was also treated as the reference molecule in the stage approximation of the exact effective molecule.

The series of activated silica studied (Table I) is particularly important in gum technology as these compounds are used as fillers in loaded pure gum compounds. Pure and nonactivated silica was studied separately, treated in part as a reference material, and its parameters [6, 7] were used in a systematic and complex analysis of internal structure.

2. Apparatus

X-ray diffractometer applied in the structural studies made by VEB Freiberger Präzisionsmechanik (GDR) is composed of a generator TuR M-62, X-ray lamp with a linear focal point, reflective graphite monochromator and a goniometer HZG-3 with a radiation counter and an electronic device for measurements and registration and for control.

The diffraction pattern of the material studies is not recorded at one moment as it is in X-ray cameras, but the course of the intensity function is obtained point after point for different angles of measurement. Therefore the demand indispensable to obtain correct results is to provide constant intensity of the primary beam. This requirement was realized by the stabilization of current and voltage in X-ray lamp in the generator TuR M-62 and by the stabilization of conditions of work of the electronic recording system. Geometer HZG-3 serves to provide necessary geometric conditions required to obtain diffraction patterns, to rotate the sample and the counter and to measure the angle of rotation which can be determined with the accuracy of $\Delta\theta = \pm 0.01°$.

The focusing system applied in a HZG-3 goniometer is after the method of Bragg and Brentano. The flat pressed powdered sample rotates with a speed two times lower than the speed of the counter so that at each position the normal to the sample surface would divide in two equal parts the angle $180° - 2\theta$, where 2θ is the angle between the incident and diffracted beam (Fig. 1). The surface of the sample is always tangent to the focusing circle passing through the source of radiation, the axis of rotation of the goniometer and the gap of the counter. Since the sample surface is tangent to the focusing circle at only one point lying on the axis of rotation of the goniometer and does not coincide with this axis some deformation in the distribution of diffracted radiation appears (broadening and shifts).

The deformations also depend on the angle of divergence of the primary beam in the horizontal plane of focusing.

The second important source of deformation in the divergence of the primary and diffracted beam operates in the vertical direction. Therefore on the path of these beams a system of gaps is placed called the Soller system of gaps. It consists of a series of thin plates of heavy metal (most often it is an alloy with lead). They are plane-parallel and the distance between them determines the vertical divergence of the beams. In a HZG-3 goniometer Soller gaps are placed on the path of the diffracted beam only, as the divergence of the primary beam in the vertical direction is considerably reduced by a system of collimation gaps.

Two methods of registration of diffracted radiation intensity are employed in the measurements performed with the X-ray diffractometer.

1. Registration by steps: the mean speed of pulse counting is recorded on the recorder tape in the time of measurement the counter moves at a con-

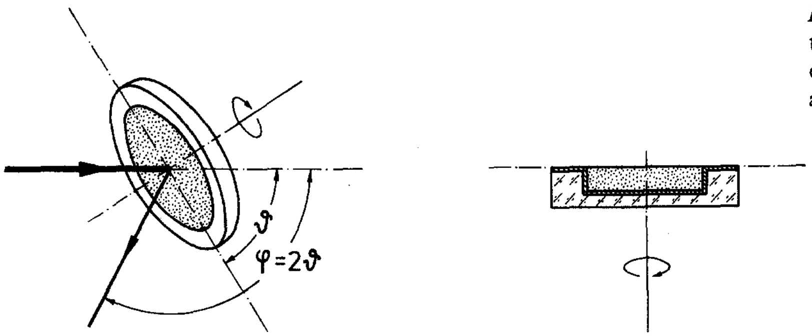

Figure 1 A schematic diagram of the measuring set-up and the cross-section of the cuvette with a specimen.

stant angular speed; the diagrams of intensity of reflection are of lower accuracy but are obtained in a relatively short time and for the whole range of angles considered.

2. Registration by jumps: automatic recording with a printer, the counter moves in jumps from one point to another and the least programmable angle between the points of measurement m and n is $\theta_{\mathrm{mn}} = 0.01°$.

3. Experiment

Large- and low-angle X-ray diffraction analysis was performed on a series of activated silica of the type $SiO_2 + R_n$ containing 2 to 3% mass fraction of the activator R_n, and on pure, nonactivated silica SiO_2 obtained chemically, dried and dehydrated by annealing at 400° C in a furnace of the vacuum apparatus.

A special method of introducing activators [11, 12] was elaborated. The studies of silica applied as a filler were performed on the mixture prepared according to the recipe for production of type treads but with 50% of carbon black replaced by silica activated with different activators. The mixtures were prepared on laboratory cylinders of a diameter of 8 cm. The cylinders were rotating with a speed of 50 turns min^{-1} and had a friction of 1:10. Next, the process of vulcanization was performed at a temperature determined by the programme of technology. From the samples obtained the paddles were cut out and they were examined for their extensibility and mechanical resistance since these parameters determine the possibility of application of silica in these products. The results obtained are given in Table I.

The silica under investigation was in a natural form of a highly granulated sample so that additional pulverization, usually needed to perform X-ray analysis, was not required.

The samples of X-ray structural studies were plane-parallel plates of naturally granulated silica formed in special cuvettes (Fig. 1) made of organic glass lined with lead foil of 1 mm in thickness. After pressing them with a steel punch in a hand press (serving for gluing microscopic optical elements and for fitting them to be plane parallel) an ideal surface for diffraction studies was obtained.

Measurements were performed by the Bragg–Brentano method [13, 14] with an automatic goniometer HZG-3 working in cooperation with an X-ray generator TuR M-62 characterized with high stability of supply current and high voltage produced by Freiberger–Präzisionsmechanik – C. Zeiss Jena (GDR).

The samples of activated silica to be investigated contained 97 to 98% mass fraction of activating compounds, R_n, of chemical composition, structure and kind of bonds with SiO_2 (forming space configurations) given in Table I. The degree of contamination with other impurities significantly influencing the structure studied was unmeasurably small. Trace impurities determined with very sensitive spectroscopic methods were almost undetectable.

Next, through numerical analysis performed by digital computer ODRA 1204 the radial functions of electron $\rho_e(r)$ and atom $\rho_a(r)$ density distribution were determined from the experimental angular functions of intensity distribution $\bar{I}(\theta)$. The experimental functions were both large and partly low-angle intensity distributions obtained for immovable and rotating sample.

All X-ray diffraction patterns were obtained at first from the record of registration potentiometer and then the data averaged over a long time of counting were gained from digital record of a line printer cooperating with the automatic goniometer.

In order to verify the correctness of angular intensity functions the measurements were repeated for each sample. Moreover, the correct-

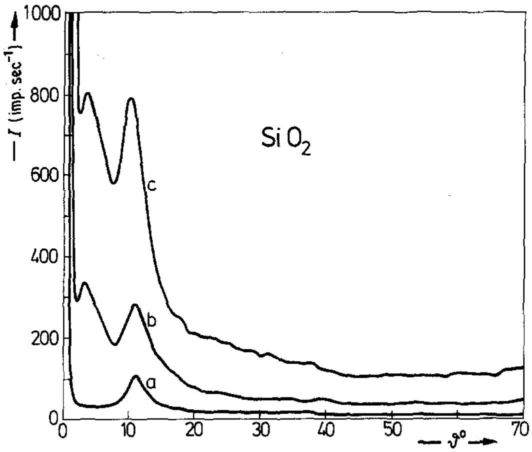

Figure 2 Angular intensity distributions of X-ray scattering in SiO_2 silica at different monochromarization: (a) nonmonochromatic radiation, (b) nickel filter, (c) graphite monochromator.

ness of the record was checked by comparing at some extreme points (for maximum and minimum intensity) the values of the function with measurements for multiplied (longer) time of counting.

In order to obtain monochromatic X-ray radiation a monochromator designed in the Laboratory of X-Ray and Electron Diffraction Structural Studies was used. The monochromator with a plane-graphite crystal ($a = 0.246$ nm, $c = 0.6760$ nm) reflecting the plane (0002) placed at an angle, $\theta = 13.45°$, to the incident beam gives efficient (coefficient of reflection at the maximum 29.3%) and well monochromatic radiation of $K\bar{\alpha}$Cu ($\lambda = 0.15418$ nm) with an integral linewidth of 48 seconds of angle (Fig. 2).

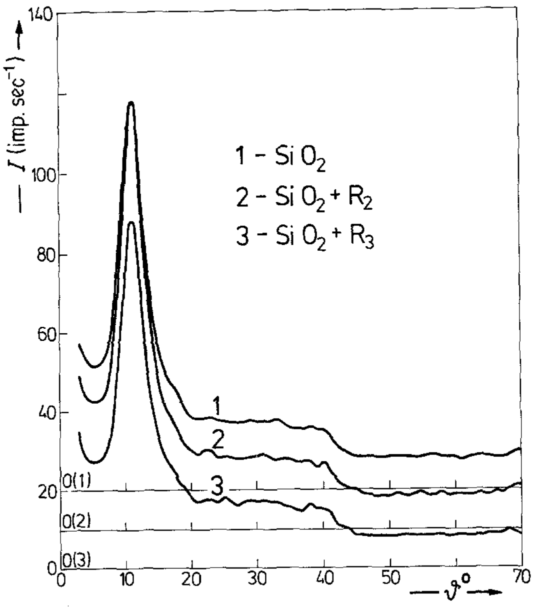

Figure 3 Angular distribution of intensity of X-ray scattering in activated and nonactivated silica.

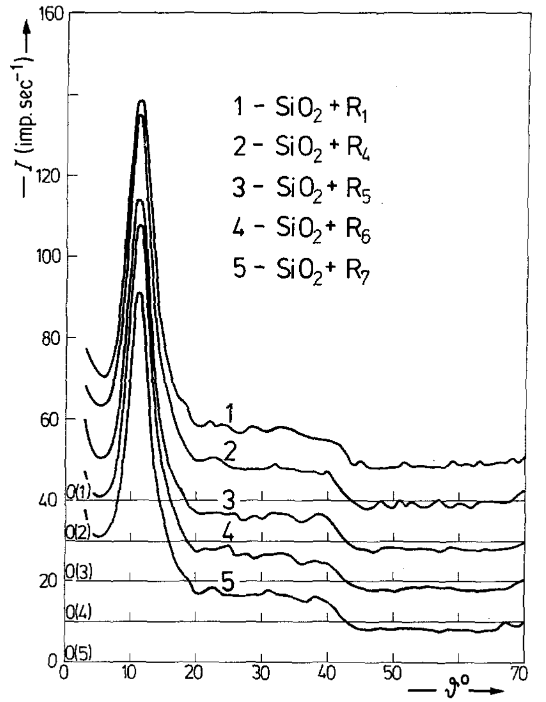

Figure 4 Angular distribution of intensity of X-ray scattering in activated silica.

The angular intensity distribution (Figs. 3 and 4) of X-ray radiation was normalized by bringing to electron units [2, 6, 7] by the digital computer method applying a special programme [15]. Each

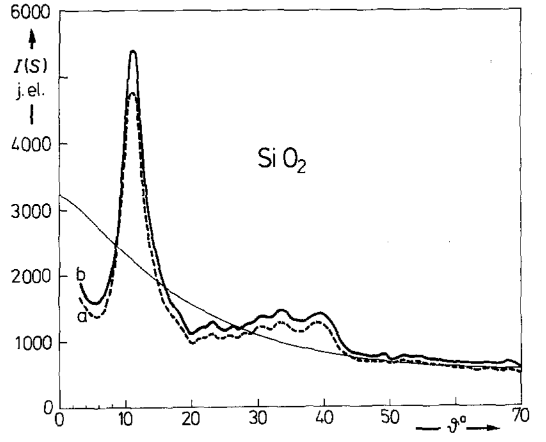

Figure 5 A comparison between the angular distributions of X-ray scattering intensity in SiO_2 silica obtained with oscillation normalization (– – –) and by the fields method (——).

function $\bar{I}(\theta)$ was normalized by the "oscillation method" or by the "area method" (Fig. 5), i.e. the oscillation of the experimental function was compared with that of the theoretical function or the areas under the experimental function were compared to those under the theoretical one. In both cases the normalization was performed for high Bragg angles of scattering, θ.

4. Theory

Quantitative structural analysis of gels to which activated and nonactivated silica belong, were performed by the method of Warren, Krutter and Morningstar [2, 10], determining radial distributions functions from the functions of angular distributions of intensity.

Direct structural analysis of silica gels (Table I) composed of $m, n, \ldots, t$ different atoms with atomic scattering factors $f_{\mathrm{m}}, f_{\mathrm{n}}, \ldots, f_{\mathrm{t}}$ and effective $K_{\mathrm{m}} = f_{\mathrm{m}}/f_{\mathrm{e}}, \ldots$ and mean effective $\bar{K}_{\mathrm{m}} = (1/S) \int_0^{S_0} K_{\mathrm{m}}\, \mathrm{d}S, \ldots$ scattering factors was carried out with the help of integral equation of Warren, Krutter and Morningstar in the form:

$$4\pi r^2 \sum_{m=1}^{t} \bar{K}_m \rho(r) = 4\pi r^2 \rho_0 \sum_{m=1}^{t} \bar{K}_{\mathrm{m}} + \frac{2r}{\pi} \int_0^{\infty} S i(S) \sin Sr\, \mathrm{d}S \quad (1)$$

From the equation in this form we can determine the function of radial distribution of electronic or atomic density $\rho(r)$. In this equation r stands for interelectron distances, $S = 4\pi \sin\theta/\lambda$, where λ is the wavelength, θ is a Bragg angle and the summation $\Sigma_{m=1}^{t}$ runs over the whole molecular unit.

Moreover the electron scattering factor is $f_{\mathrm{e}} = \Sigma_{m=1}^{t} f_{\mathrm{m}} / \Sigma_{m=1}^{t} Z_{\mathrm{m}}$ where $Z_{\mathrm{m}}, Z_{\mathrm{n}}, \ldots, Z_{\mathrm{t}}$ stands for atomic numbers.

The mean electron density is expressed by

$$\rho_0 = dN_{\mathrm{A}} 10^{-24} \sum_{m=1}^{t} \bar{K}_n/M = dN_{\mathrm{A}} 10^{-24} \sum_{m=1}^{t} \bar{Z}_n/M \quad (2)$$

where N_{A} is the Avogadro number, d is the macroscopic density and M is the molecular mass expressed in physical units.

Taking into account the corrections for polarization, absorption, incoherent radiation, nonlinear registration of intensity, geometry of the measuring system, normalization of the function, mean values of $\bar{I}(S)^{\mathrm{EXP}}$ measured experimentally take the values $\bar{I}(S)^{\mathrm{COH}}$ being the components of the expression:

$$i(S) = \left[\bar{I}(S)^{\mathrm{COH}} \Big/ N - \sum_{m=1}^{t} f_{\mathrm{m}}^2 \right] \Big/ f_{\mathrm{e}}^2 \quad (3)$$

$$= \sum_{m=1}^{t} Z_{\mathrm{m}} \left[\bar{I}(S)^{\mathrm{COH}} \Big/ N \sum_{m=1}^{t} f_{\mathrm{m}}^2 - 1 \right].$$

Both approximate parameters of nodal structure: $\bar{a}_1, \bar{a}_2, \bar{a}_3, \ldots, \bar{a}_{\mathrm{n}}$ (introduced to describe simple models of atomic–molecular systems of noncrystalline substances [3, 4, 6, 7]) and parameters of radial distribution: $\bar{r}_1, \bar{r}_2, \bar{r}_3, \ldots, \bar{r}_{\mathrm{n}}$ correspond to the distances between atoms and atom groups occurring in the silica studied. The parameters $\bar{a}_1, \bar{a}_2, \bar{a}_3, \ldots, \bar{a}_{\mathrm{n}}$ describe a general and aperiodic nodal lattice which can be ascribed to the silica studied while the parameters $\bar{r}_1, \bar{r}_2, \bar{r}_3, \ldots, \bar{r}_{\mathrm{n}}$ correspond only to the calculated distances obtained by Fourier analysis from the radial distribution function.

Thus, we obtain only the distance parameters which can be ascribed to the model of internal structure of silica; the more so as only a part of the parameters calculated from the radial distribution function correlate with the constants of aperiodic nodal lattice which is of more general character.

For the studied series of activated silica interatomic and intermolecular distances correlate well with the functions of radial distribution $\rho(r)$: $\bar{r}_1 \cong 0.162$ nm, $\bar{r}_2 \cong 0.280$ to 0.290 nm, $\bar{r}_3 \cong 0.404$ to 0.412 nm, $\bar{r}_4 \cong 0.510$ to 0.512 nm and [$\bar{r}_5 \cong 0.615$ to 0.620 nm].

Similarly good correlation is found for the functions of angular distribution of intensity obtained from the corrected Bragg equation [2, 6]:

$$R = 1.25 \times d_{\mathrm{Bragg}} \quad (4)$$

derived from the analysis of the Debye function [2, 5] in the form:

$$I(S) = Nf^2 \sum_{m=1}^{t} \frac{\sin Sr_{\mathrm{mn}}}{Sr_{\mathrm{mn}}} \quad (5)$$

In this way the approximated parameters are found: $\bar{a}_1 \cong 0.17$ nm, $\bar{a}_2 \cong 0.29$ nm, $\bar{a}_3 \cong 0.41$ nm, $\bar{a}_4 \cong 0.51$ nm and [$\bar{a}_5 \cong 0.62$ nm]. They correspond to the subsequent least distances in the space aperiodic nodal model with partial internal ordering.

5. Structural analysis of activated silica

The structure of nonactivated and activated silica of the type $SiO_2 + R_n$ was investigated, for different degrees of activation and different activators. The distribution of intensity of monochromatic radiation Cu*Kα* ($\lambda = 0.154\,18$ nm), obtained for the series of silica studied did not reveal any noticeable difference in the whole range of θ considered, ($1° < \theta < 70°$), (Figs. 3 and 4) illustrates the influence of degree of monochromatization of X-ray radiation of diffraction pattern of pure silica. The more monochromatic the radiation is the more sharp and clear is the pattern obtained and the less apparatus background appear spectral background becomes eliminated. After the corrections had been introduced and normalization to electron units performed we chose three samples A-002, A-003, and A-008, for further numerical analysis (Fig. 6).

The summarized (Fig. 7) and differentiated (Fig. 8) curves of radial distribution functions, calculated from the experimental angular intensity distributions, correspond to the distances between silicon, oxygen and hydrogen atoms, which are identical for nonactivated and activated silica [6, 7].

The influence of an activator in an amount of 2 to 3% mass fraction does not cause any noticeable change in the structure of silica analysed in the regions of 0.6 to 1 nm.

Therefore, similarly as for pure silica we can treat the first maximum for $r = 0.162$ nm as corresponding to distances of 0.160 nm between silicon and oxygen. The distance is the repeatable parameter in the oxide–silicon skeleton in crystalline silica [16]. The position of the maximum covers the range from 0.12 to 0.19 nm only slightly depends on the degree of activation of silica. The second maximum, sharply distinguished for $r = 0.280$ to 0.290 nm covers the range from 0.25 to 0.32 nm. This range corresponded only in part to the distance of 0.258 nm between oxygen atoms O^I–O^I in an oxide–silicon tetrahedron and it partly corresponds to the distances of 0.32 nm Si–O–Si between silicon atoms, belonging to the neighbouring oxygen tetrahedra and lying on the same line.

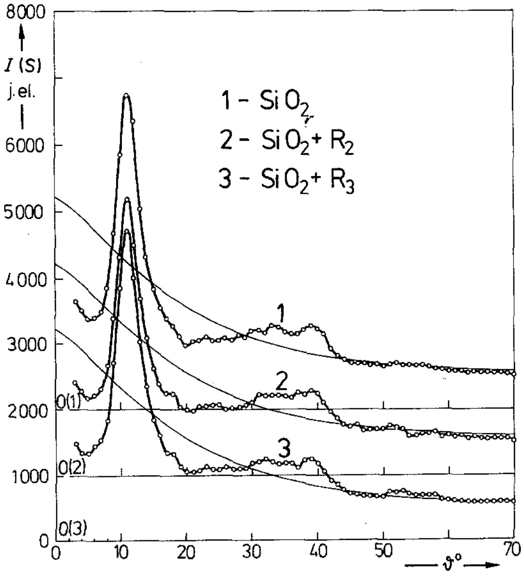

Figure 6 Angular distribution of X-ray scattering intensity in activated and nonactivated silica after normalization.

There is no high-ordering in both nonactivated and activated silica. In silica, some traces of oxide–silicon tetrahedra are found, which causes the distance between silicon ions belonging to two neighbouring cells to be always less than the maximum distance of 0.32 nm.

The third maximum for $r = 0.404$ to 0.412 nm corresponded to the two inseparable maxima at 0.40 and at 0.45 nm due to the distances between individual atoms Si^{II}–O^{II} and O^I–O^{II} belonging to neighbouring tetrahedra. The fourth maximum found for $r = 0.510$ to 0.512 nm (in the region from 0.48 to 0.54 nm) for all radial distributions analysed, corresponds to the distances between silicon atoms belonging to the two neighbouring tetrahedra not directly adjacent [7, 1].

For interatomic distances greater than 0.6 nm we cannot unequivocally establish structural parameters and ascribe them to the atom groups analysed due to mutual reorientation of the tetrahedron groups. Further structural analysis of activated silica, which would enable construction of a space model and finding the probability of space distribution of activator groups, would also allow us to find local groups in internal ordering [1]. In this regard the authors consider as very promising the results of X-ray structural analysis performed by the low-angle diffraction method.

6. Conclusions

The positions of maxima and minima obtained from Fourier analysis on the curves of summarized and differentiated functions of radial distribution of electron density, determine the probability of finding the particular interatomic and intermolecular distances.

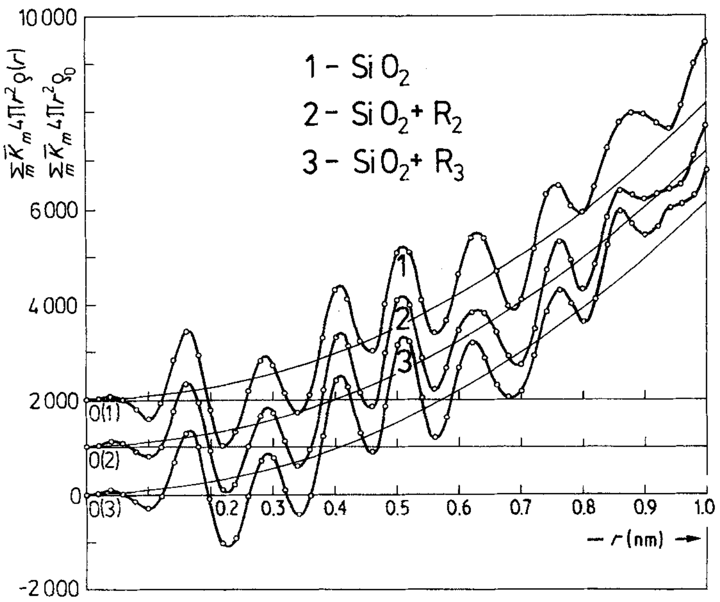

Figure 7 Summary functions of radial distributions for silica.

On the curve of the radial distribution function for the silica studied (Figs. 7 and 8), seven clearly distinguished maxima are found in the range from 0 to 1.0 nm. The first five of them give essential information on internal structure. For distances greater than 0.6 nm it is hard to correlate unequivocally the maxima with interatomic or intermolecular distances [1].

The subsequent maxima correspond to the interference due to molecules at still longer distances. The results obtained prove that the local structure of activated and nonactivated silica is the same. Groups of an activator do not change the structure of silica noticeably. The presence of activators is not revealed in the course of the angular distribution of intensity.

Detailed quantitative analysis of electron density on the grounds of integration of the area limited by the function and the x-axis allows the establishment of a structural model of pure and activated silica [1] by a trial and error technique, a degree of ordering in larger regions and, possibly, to find the positions of activator groups.

The analysis performed supports the thesis of

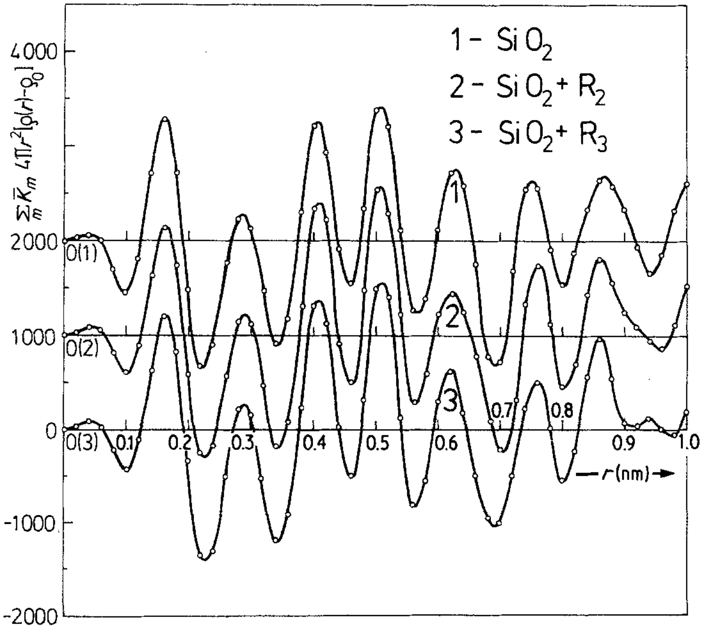

Figure 8 Differential funcations of radial distribution for silica.

tetrahedral configuration of silicon with respect to oxygen atoms in silica: $SiO_2 + R_n$, independently of a degree of activation and the structure of an activator R_n. Thus, we suppose that the configuration of the R_n molecules both with respect to one another and to the oxide–silicon skeleton in similar to that of the distorted tetrahedra [7, 1, 17].

Regarding the noncrystalline structure of the silica series studied, the distances (the lengths of the vectors) between the extreme oxygen atoms $\overline{\mathrm{O{-}Si{-}O}}$ and extreme silicon atoms $\overline{\mathrm{Si{-}O{-}Si}}$ of the neighbouring tetrahedra depend on the change in space configuration and on reorientations of individual tetrahedra about the axis Si–O–Si running through the centres of these atoms. Interatomic distances in the region from 0 to 0.6 nm have been determined with satisfactory accuracy and correlate well with the results of other authors [18–20].

References

1. Z. BOCHYŃSKI, S. MOCYDLARZ, *Szkło i Ceramika* **34** (1982), in preparation.
2. H. P. KLUG and L. E. ALEXANDER, "X-Ray Diffraction Procedures for Polycrystalline and Amorphous Materials" (John Wiley, New York, 1966).
3. Z. BOCHYŃSKI, *Normalizacja* **45** (1977) 25.
4. *Idem, ibid.* **45** (1977) 23.
5. R. W. JAMES, "The Optical Principles of the Diffraction of X-Rays" (Bell and Sons, London, 1948).
6. Z. BOCHYŃSKI, "Study of the Structure and of the Internal Ordering Degree in Inorganic Oxide Glasses" (Scientific Publishers UAM, Poznań, 1980) (in Polish).
7. *Idem, PTPN, Fiz. Dielek. Radiospektrosk.* **14** (1983) in press.
8. *Idem, ibid.* 7 (1975) 187.
9. N. C. ANDREJEW, O. W. MAZURIN, E. A. PORAI-KOSHITS, G. P. ROSKOVA and W. N. FILIPOWICZ, "Yavlenya likvatsii w styoklak" (Nauka, Leningrad, 1974) p. 53.
10. Z. BOCHYŃSKI, *PTPN, Fiz. Dielek. Radiospektrosk.* **9** (1977) 229.
11. S. MOCYDLARZ, Patent PRL Nr 137819 (1980).
12. S. MOCYDLARZ and B. RAGER, *Przemysł Chemiczny* **56** (1980) 14.
13. A. GUINIER, 'Théorie et Technique de la Radiocristallographie" (Dunod, Paris, 1956).
14. W. LÖSCHAU, K. MORAS, R. BÖTTGER, M. LANGER and K. MAYER, *Jenaer Rundschau* **23** (1978) 160.
15. Z. BOCHYŃSKI, J. BUCHERT and R. MATUSZEWSKI, *PTPN, Fiz. Dielek. Radiospektrosk.* in preparation.
16. B. K. WAJNSZTEJN and A. A. CZJERNOW (eds) "Probljemy Sowrjemjennoj Kristałłografii" (Nauka, Moscow, 1975).
17. S. MOCYDLARZ, J. FIAŁ, S. OLKIEWICZ and M. TOKARZ, *Przemsł Chemiczny* **57** (1981) in press.
18. B. E. WARREN, H. KRUTTER and O. MORNINGSTAR, *J. Amer. Ceram. Soc.* **19** (1936) 202.
19. B. E. WARREN, *J. Appl. Phys.* 8 (1937) 645.
20. M. A. BJEZBORODOW, "Sintez i Strojenije Silikatnych Stjekoł" (Nauka i tjechnika, Mińsk, 1968) pp. 227, 341.

*Received 22 July
and accepted 29 July 1983*